ATTENUATION CORRECTION IN CARDIAC SPECT USING CONSISTENCY CONDITIONS

Ana Maria Marques da Silva[*a], *Cecil Chow Robilotta*[b]

[a]Physics Institute, PUCRS, Porto Alegre, Brazil;
[b]Physics Institute, USP, São Paulo, Brazil.

ABSTRACT

In this work the approach for obtaining the attenuation maps for cardiac SPECT was the estimation directly from the emission data, without transmission imaging, based on consistency conditions of the attenuated Radon transform. Several counting rates and attenuation coefficients on the corrected images were studied, using the MCAT phantom and SimSET package. Given an initial estimate of the attenuation map, the use of consistency conditions always resulted in a same form, for any values initials of the group of parameters. In spite of the fact that the error falls with the increasing counting rate, higher counts are not able to determine the best attenuation coefficient. The results shows that consistency conditions can be useful for attenuation correction, but the scattering correction is the most important factor in the quantitative reconstruction in cardiac SPECT.

1. INTRODUCTION

The main objective of quantitative SPECT is to supply reconstructed images where the value of each pixel represents the activity in the corresponding area of the patient. To quantify SPECT images, it is necessary to eliminate the effects of degrading factors, without introducing distortions and artefacts. As this is not possible, it is attempted then to minimise those effects. Thus, studies of attenuation correction methods, scattering and other degrading factors of SPECT help to minimise the difficulties and to reach the final aim of a more accurate quantification [1].

Among the attenuation correction methods, a current tendency consists in obtaining an attenuation coefficient map of the object through transmission imaging. A completely different approach was proposed by Natterer [2], where the attenuation map is obtained without the additional acquisition of transmission images, which also avoids problems associated with the registration of images of different modalities. This method is based on the application of consistency conditions of the attenuated Radon transform to estimate the attenuation map from the emission projections.

Researchers [3,4] tested the method on simulated images of uniform and non-uniform attenuating regular geometrical objects in SPECT, as well as on attenuation correction in PET [5].

In this work, we applied the method derived by Natterer on simulated cardiac SPECT images and studied the influence of counting rate and the dependence on different attenuation coefficients. The MCAT phantom [6] with different attenuating tissues was employed in the simulations and attenuation corrected images were reconstructed using an iterative ML-EM algorithm with a projector-backprojector modified by the attenuation map [7]. Quantification was then performed in the myocardium for evaluation of the correction methods.

2. MATERIALS AND METHODS

2.1. Emission Data

Monte Carlo methods are used intensively to study the photon transmission and scattering through homogeneous and heterogeneous objects in radionuclide tomography, as separated primary and scattered photons can be generated in different projection groups [8].

In the present work we have adopted, for generating the emission projections, SimSET package [9]. The MCAT phantom filled with ^{99m}Tc used in our simulations has the following dimensions: 40 cm lateral width, 30 cm antero-posterior length and 40.32 cm height. The 128 projections in 360 degrees were simulated for matrices of 64×64 pixels of 6.3 mm. The acquisition window was 127 to 154 keV.

* ana.marques@pucrs.br; phone 55 51 3320-3682; fax 55 51 3320-3616;
http://www.pucrs.br/fisica/pesquisas/nimed/index.htm

Primary and scattered photons images were generated separately. The energy resolution considered was 13% (FWHM) for 140 keV. The LEHR collimator with parallel holes (32.8 mm length, 1.4 mm hole diameter and 0.152 mm septal thickness) was used.

The specific activity in the myocardium was fixed in 50 μCi/cm^3. Other activities were assigned as fractions of that value: myocardium =1, spleen = 0.96, kidneys = 0.84, liver = 0.69, blood/soft tissue = 0.09 and lung = 0.03 [10].

2.2. Reconstruction Method

The maximum-likelihood expectation-maximization (ML-EM) iterative method was used for the reconstructions. The attenuation correction was incorporated into the reconstruction algorithm during the projection and backprojection operations. Scatter and geometric response corrections were not included in the reconstruction algorithm.

2.3. Determination of attenuation map using consistency conditions

Some researchers [4] calculate simultaneously the attenuation map and activity distribution directly from emission data, through the solution of a set of equations that govern the image formation process in SPECT. The main problem of these methods is that attenuation and activity distributions are intimately related in the image equations. It is very difficult to solve one distribution unless the other distribution is known a priori.

Natterer [2] demonstrated that the attenuated Radon transform should satisfy a set of consistency conditions, derived from the Helgason-Ludwig conditions (or moments conditions). These equations can be used to estimate the attenuation map directly from the emission sinograms. The attenuation map and the activity distribution can be numerically determined, if general information about these distributions, like an initial guess for the attenuation map, are known a priori.

Natterer's formulation of Helgason-Ludwig conditions for the general case of SPECT are [2]:

$$\int_0^{2\pi} e^{ik\varphi} \int_{-\infty}^{\infty} s^m e^{\frac{1}{2}(T(\theta,s)+i\mathbf{H}T(\theta,s))} g(\theta,s)\,ds\,d\varphi = 0, \quad (1)$$

where s is the detector bin; θ is the angle projection where $\theta = (\cos\varphi, \sin\varphi)^T$; m is the moment order and k is an integer, with $0 \le m < k$; $g(\theta, s)$ represents the measured data or emission sinogram (attenuated Radon transform of activity distribution); $T(\theta, s)$ represents the transmission sinogram (non-attenuated Radon transform of the attenuation distribution); **H** represents the Hilbert transform operator that acts on $T(\theta, s)$ as a function of s.

The central part of equation (1) is the equation of the m moment, which is dependent of the position s. If the data satisfy the Helgason-Ludwig conditions, this equation will yield a sum of sine waves with whole periods not greater than m. The multiplication of this central part by e^{ik} and integration over φ is equivalent to taking the dot product of two sine waves with different whole periods that should be equal to zero.

If $g(\theta, s)$ is supplied by the measured emission data of a SPECT system, then the consistency conditions become a set of nonlinear equations for the unknown transmission data $T(\theta, s)$. Details of consistency conditions equations can be found in Natterer [11].

The method proposed by Natterer demands that the attenuation distribution is known through affine transformations (translation, rotation and scale) of an initial guess-attenuation-map. In this work, a uniform circle with a given constant attenuation coefficient was used. As the attenuation map is a distortion of the initial uniform attenuation map, the modified projection will only depend on the values of the affine transformation. The parameters A and b of an affine transformation can be appraised through a non-linear least-squares minimisation routine without constraints, such as the Levenberg-Marquardt method. The routine will determine the values of A and b that supply the best adjustment to the consistency conditions, when applied to the initial attenuation distribution. The goodness-of-fit of data is assessed by the sum of the Fourier coefficients greater than m, which ideally should be zero. This sum will be called in this text the error of the consistency conditions. The values of the parameters determined after the convergence are used to distort the sinogram of the initial attenuation map. The evaluation of the consistency conditions was performed through the program ConTraSPECT that searches for the attenuation map more consistent with the emission sinogram, implemented by Welch [5].

The analysis developed in the present work explores two aspects of the method on estimating the attenuation map from the consistency conditions in SPECT: (i) the acquisition counting rate in the convergence of the method; (oi) the value of attenuation coefficient in the initial estimation of a free shaped attenuator and

3. RESULTS AND DISCUSSION

The effects of the acquisition counting statistics on the accuracy of the estimated attenuation map was evaluated using the consistency conditions in four simulations of the MCAT emission sinogram, with the following total counts: 2.3×10^7 (maximum value = 178 counts/pixel); 1.1×10^7 (maximum value = 106 counts/pixel); 5.7×10^6 (maximum value = 58 counts/pixel) and 2.3×10^6 (maximum value = 27 counts/pixel). In general, the error of consistency conditions decreases with increase of total count, but does not bias the

estimated parameters. This result is reasonable, as the noisy nature of the emission sinogram is not considered in the consistency equations. The evaluation of errors as function of total count leads to the conclusion that the method is quite robust, resulting in solutions with errors smaller than 3%. These results are also confirmed for PET data [5].

The estimation of the attenuation map using consistency conditions was accomplished for the 1.1×10^7 counts (maximum value = 106 counts/pixel) emission sinogram, representing routine clinical cardiac studies. The results presented from this point onwards will always be referred to this total count. The visual analysis of the estimated attenuation maps from the consistency conditions, compared to the perfect non-uniform attenuation maps, leads to some conclusions regarding the method. Figures 1 shows the estimated maps for different values of attenuation coefficients, in a slice that contains the myocardium, only considering the primary photons, overlaid onto the perfect non-uniform maps.

The estimated maps are not distorted equally in all directions; they present a larger displacement for small lung area that corresponds to a higher effective attenuation coefficient area. The estimated maps for larger attenuation coefficients, as 0.15 and 0.16 cm^{-1}, are smaller than the body actual contour. This is due to the fact that the solution found by the consistency equations to fit a uniform map, in order to compensate for an "average" smaller attenuation coefficient, derived from large lung areas. The consistency conditions do not find, in that case, a uniform map consistent with the emission data and adjusted to the body contour. In other words, the use of a uniform attenuation map with the body contour is inconsistent with the emission data in the considered situations.

In slices where estimated maps are smaller than the body contour, areas that are "outside" the map are not corrected properly. However, these areas are usually limited to the borders of the lungs, with less important clinical interest. The area of higher activity in such slices (myocardium) is always contained inside the estimated attenuation map and it is properly corrected.

For images reconstructed with the primary photons, the attenuation coefficient that results in the best quantitative fitting is 0.14 cm^{-1}. This value was obtained by the smallest difference between ideal and corrected image.

One example of myocardium slice (33) was used for evaluation and the result is shown in Figure 2. The map estimated by consistency conditions considered for the attenuation correction has μ = 0.14 cm^{-1}. The comparison includes the reconstructions of the slice using uniform map limited by body contour (μ = 0.12 cm^{-1}). Only the primary photons were used in the reconstructions.

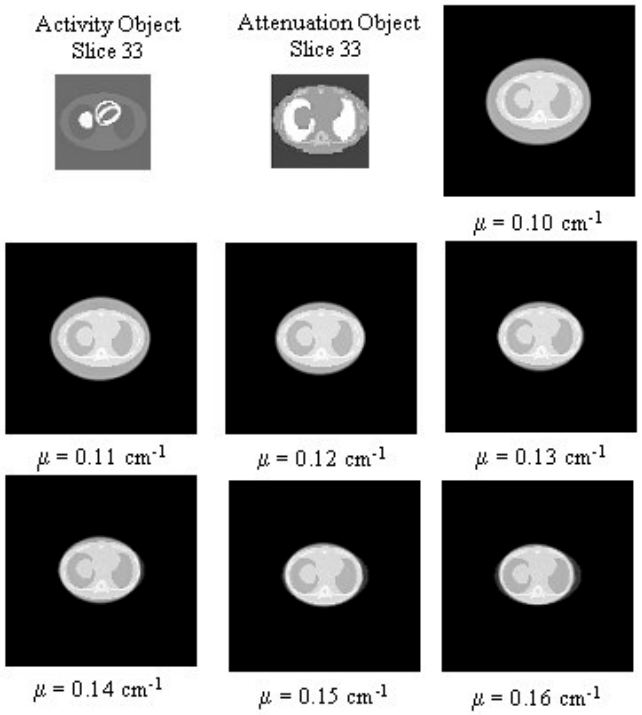

Fig 1 - The slice shown are the high asymmetry of the non-uniform activity distribution and the non-uniformity of the original attenuation map.

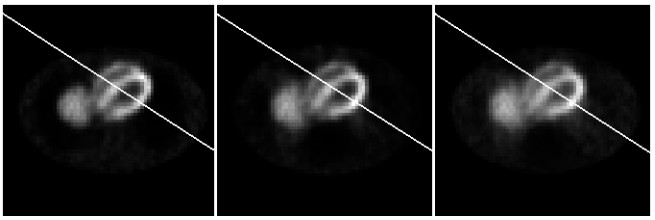

(a) (b) (c)

Fig. 2 – Reconstructed profiles of slice 33 only with primary photons: (a) ideal, without attenuator; (b) attenuation correction using the consistency conditions (μ = 0.14 cm^{-1}); (c) attenuation correction using uniform map (μ = 0.12 cm^{-1}).

The count profiles of the images reconstructed only with primary photons show that the correction preserves the wall thickness (Figure 3). The attenuation correction does not show the loss of contrast between cavities and walls. The myocardium posterior wall is over-corrected in slice 33. The final result of the total counts in the slices corrected with μ = 0.14 cm^{-1} generated a myocardium image with a total value very close to the ideal one.

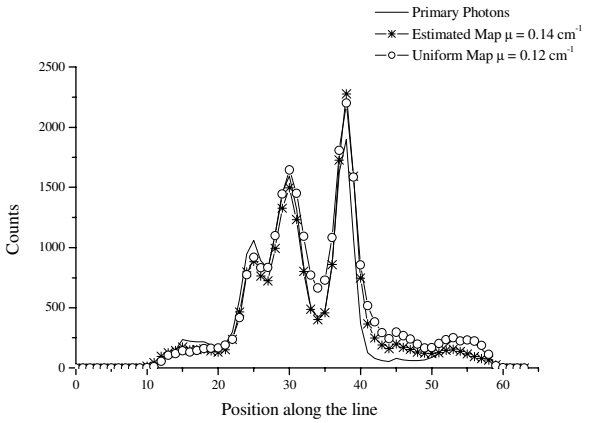

Fig. 3 - Comparisons of profile indicated in Figure 2 of slice 33, when only primary photons are considered:

The estimated maps with the inclusion of scattered photons are usually smaller than those estimated with only the primary photons, if the same μ is used, confirming the results obtained by Welch and collaborators [5]. The best solution in consistency conditions, using scattered photons is obtained with a smaller value of μ (0.12 cm^{-1}). This is coherent with the use of an effective μ, body-limited, to correct attenuation and scattering. However, the correction using this estimated attenuation map does not get to compensate properly the scattering.

The inefficiency of this method in correcting the emission data that include scattered photons can be explained by the fact that the consistency conditions only take into account the effect of attenuation in their theoretical formulation, without any reference to the scattering of emitted photons. This lack of sensitivity for the scattered events in the estimation of the attenuation map is revealed in the small modification of the dimensions of the estimated map.

These results point to the fact that use of consistency conditions to estimate the attenuation map will only produce quantitatively acceptable results if appropriate scattering correction is accomplished first.

4. DISCUSSION AND CONCLUSIONS

The present work estimated the attenuation map consistent with a non-uniform radioactive distribution, formed by several active volumes in a non-uniform attenuating medium, such as the MCAT phantom. Four statistical situations with different total counts and coefficients of attenuation in the initial estimation of the attenuation map were considered.

The results showed that consistency conditions always lead to the same final attenuation map for each slice, from any initial uniform map. The correction generated the same artefacts produced by correction with body contour uniform map, such as stretches of high activity in the lungs and an area of less activity in the central region of the back, near the spine. Such artefacts are particularly intense in the slices near or containing the liver. However, free distortion allowed a better correction in slices distant from the liver and a better quantification of myocardium activity, when compared to correction using a body contour uniform map.

The inclusion of scattered photons in the emission sinogram modified the solution of the consistency equations, moving the attenuation value to smaller ones than those obtained with only primary photons. For a same value of μ, the estimated attenuation map with the inclusion of the scattered photons was slightly smaller than the one estimated with the primary photons. However, the estimated map does not correct properly the scatter in the myocardium, particularly in the liver area.

The results from the present studies indicated that the use of consistency conditions to estimate the attenuation map would only produce quantitatively correct images if appropriate scattering corrections were accomplished before the application of the method.

5. REFERENCES

[1] B.M.W. Tsui, et al.," Quantitative Single-Photon Emission Computed Tomography: basics and clinical considerations", *Semin. Nucl. Med.,* XXIV pp. 38-65, 1994.

[2] F. Natterer, "Determination of tissue attenuation in emission tomography of optically dense media", *Inverse Problems*, 9, pp. 731-736, 1993.

[3] A.S. Welch, et al., "Toward accurate attenuation correction in SPECT without transmission measurements", *IEEE Trans. Med. Imag.*, MI-16(5), pp. 532-541, 1997.

[4] A. Krol, et. al, "An EM Algorithm for Estimating SPECT Emission and Transmission Parameters from Emission Data Only", *IEEE Trans. Med. Imag.*, MI-20(3), pp. 218-232, 2001.

[5] A.S. Welch, et al., "Attenuation Correction in PET Using Consistency Information", *IEEE Trans.Nucl.Sci*, 45(2), pp.3134-3141, 1998.

[6] K.J. LaCroix, "Evaluation of na attenuation compensation method with respect to defect detection for ^{99m}Tc-sestamibi myocardial SPECT images", *PhD Thesis*. UNC Chapel Hill, 1997.

[7] G.T. Gullberg, et al., "An attenuated projector-backprojector for iterative SPECT reconstruction", *Phys. Med. Biol.* 30(8), pp. 799-816, 1985.

[8] H. Zaidi, "Relevance of accurate Monte Carlo modeling in nuclear medical imaging", *Med Phys.,* 26(4), pp. 574-608, 1999.

[9] T.K. Lewellen, et al., "Design of a simulation system for emission tomographs", *J.Nucl.Med.,* 29, pp. 871, 1988.

[10] M. A. King, et al., "Attenuation compensation for cardiac single-photon emission tomographic imaging: Part 2. Attenuation compensation algorithms", *J.Nucl.Cardiol.,* 3, pp. 55–63, 1996.

[11] F. Natterer, "*The Mathematics of Computerized Tomography",* John Wiley, 1986.